Investigation of Subharmonic Mixer Based on a Quantum Barrier Device

W. Y. Liu, *Member, IEEE,* and David Paul Steenson, *Member, IEEE*

***Abstract*—This paper presents our findings on novel subharmonic mixers using quantum barrier devices. These devices appear to be ideally suited to terahertz operation because of their highly nonlinear and predictable characteristics. Analytical evidence, together with experimental proof-of-principle results, is presented for a quantum-barrier-device mixer in order to demonstrate the result of intrinsic effects that effectively control the device nonlinearities and, therefore, the mixing performance. Such behavior is not found in Schottky junctions, and can be used to provide efficient subharmonic operation at terahertz frequencies with the significant advantage of permitting the use of very low levels of local-oscillator power.**

***Index Terms*—Quantum barrier device, subharmonic mixer.**

I. Introduction

TODAY, subharmonic mixers are widely employed as down-converters at millimeter- or submillimeter-wave frequencies, primarily because this type of mixers perform reasonably well with local oscillators (LO's) of lower frequency. The most common type of subharmonic mixer is the Schottky-based second harmonic mixer. The subharmonic mixer is normally realized in a pair of Schottky diodes connected in antiparallel, the purpose of which is to suppress the fundamental mixing that will otherwise reduce the power available for second subharmonic mixing. Although two diodes connected in antiparallel is conceptually simple, any mismatch in the physical and electrical characteristics between the two diodes will potentially waste the LO power that could otherwise be used for the desired harmonic components.

Alternatively, a much more attractive solution is to replace the pair of antiparallel diodes with a single quantum barrier device (QBD) [5], [6], [8], [9], which has a highly nonlinear and antisymmetric conductance. In this way, the antisymmetric conductance intrinsic to this type of device can effectively suppress the fundamental mixing in a subharmonic mixer design. This is just one of the advantages that justify the use of a single QBD in realization of a subharmonically pumped mixer.

Another advantage attributed to the QBD is that this class of devices contains multiple barriers arranged in series. The barrier width and interbarrier spacing can be tailored in such a way that the unbiased capacitance can be minimized. The unbiased capacitance normally contributes negative effects to the overall mixing performance. In a mixer operating in terahertz frequencies, at which the unbiased capacitance becomes a dominant factor, QBD's appear to be a more flexible device than the Schottky junctions in this respect.

Primarily though, it is the fact that the barriers of a QBD can be tailored during fabrication in such a way that the nonlinearities associated with the device can be brought under control to favor either high- or low-power pump requirements. It is also possible to choose different layer structures for a device of the same diameter to obtain optimum resistive nonlinearities. Flexibility to modify the nonlinearities at a device level or in terms of the transmission coefficient resulting from quantum interference effects, together with the flexibility to modify the electron distribution in the emitter (i.e., the supply function) means a flexibility to tailor the nonlinear behavior to favor different operating conditions. This is the primary advantage of using QBD's as submillimeter-wave subharmonic mixers.

The excellent intrinsic mixing performance has been reported previously in [6], [8], and [9]. In addition, Tait [8] has also identified other advantages of a heterojunction barrier device suitable for millimeter-wave mixer design, including the opportunities to fabricate low-barrier-height structures that reduce the LO power requirements and to improve device reliability under both continuous-wave and pulsed-power operation. This has been experimentally demonstrated by the authors using a QBD in an another similar experiment [9], in which a conversion of less than 9 dB was achieved for an 18–0.9-GHz subharmonic mixer using a double barrier device in the absence of any dc bias. Mixing with conversion gain at the W-band has also been demonstrated as being possible when biased negatively or positively to the negative dynamic resistance region [8]. These results show that superior mixing performance of a QBD at microwave or millimeter frequencies is without doubt. However, there has yet been any research performed that analytically verifies the essential features of the barrier devices that Schottky devices cannot offer.

In the following sections, the basic mixing mechanism in a nonlinear network is reviewed, with particular reference given to the electrical behavior of a QBD. A more qualitative treatment will be given to identify the essential differences between the barrier and Schottky diodes.

II. Qualitative Treatments

In this section, the frequency-conversion mechanism of a mixing device is qualitatively reviewed. Our derivation will be based on an arbitrary nonlinear device that can be understood as a combination of a nonlinear capacitor and a nonlinear resistor connected in parallel, as shown in the equivalent model of Fig. 1. The series impedance intrinsic to the device is assumed to be incorporated into the external network.

Manuscript received March 30, 1999. This work was supported by the Engineering and Physical Sciences Research Council, U.K., under Contract GR/L/43633 and Contract GR/E/91 325.

The authors are with the School of Electrical Engieering, The University of Leeds, Leeds LS2 9JT, U.K.

Publisher Item Identifier S 0018-9480(00)02537-0.

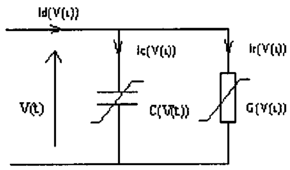

Fig. 1. Equivalent circuit of a nonlinear diode.

Under two-tone modulation, a nonlinear device is simultaneously excited by the two time-dependent sinusoidal signals, namely, the RF signal $V_{\mathrm{RF}}(t) = V_{\mathrm{rf}} \cos(w_{\mathrm{rf}} t)$ and the LO pump $V_{\mathrm{LO}}(t) = V_{\mathrm{lo}} \cos(w_{\mathrm{lo}} t)$. In the absence of any bias, by superimposition in the time domain, the voltage across the diode junction is given as

$$V(t) = V_{\mathrm{rf}} \cos(\omega_{\mathrm{rf}} t) + V_{\mathrm{lo}} \cos(\omega_{\mathrm{lo}} t) - V_{\mathrm{if}} \cos(\omega_{\mathrm{if}} t + \psi_{\mathrm{if}}) \tag{1}$$

where $\omega_{\mathrm{if}} = \omega_{\mathrm{rf}} - k\omega_{\mathrm{lo}}$ and $V_{\mathrm{if}} \cos(\omega_{\mathrm{if}} t + \psi_{\mathrm{if}})$ represents the IF voltage $V_{\mathrm{IF}}(t)$ due to the termination impedance at the IF terminal. k can be any nonzero integer.

A. Resistive Mixing

The nonlinear resistance of a diode can be modeled as a voltage-controlled current generator, with the nonlinear I–V relationship given as a multiorder polynomial

$$I_r(t) = \sum_{j=0}^{\infty} a_j V(t)^j. \tag{2}$$

Assume that, as in the normal situation, the LO voltage is very much greater in magnitude than the RF signal. Under a resistive mixing condition, where conversion loss is a norm, it is reasonable to assume that

$$V_{\mathrm{lo}} \gg V_{\mathrm{rf}} > V_{\mathrm{if}}. \tag{3}$$

Applying Taylor expansion on (2) about $(V_{\mathrm{RF}}(t) - V_{\mathrm{IF}}(t)) = 0$, and because of the assumption made in (3), the resistive current can be reasonably approximated as

$$ir(t) \approx \sum_{i=0}^{\infty} a_i V_{\mathrm{LO}}(t)^i + \frac{1}{2} \sum_{i=0}^{\infty} i a_i V_{\mathrm{LO}}(t)^{i-1} \Big(V_{\mathrm{RF}}(t) - V_{\mathrm{IF}}(t)\Big). \tag{4}$$

In the foregoing analysis, the formula of (5) will be used to extract a particular harmonic of the LO signal

$$\Big(V_{lo} \cos(\omega_{lo} t)\Big)^i = \frac{V_{lo}^i}{2^{i-1}} \binom{i}{i + \frac{k}{2}} \cos(k\omega_{lo} t) + \frac{V_{lo}^i}{2^i} \sum_{\substack{r=0 \\ r \neq \frac{i \pm k}{2}}} \binom{i}{r} e^{j\omega_{lo}(2r-i)t} \tag{5}$$

where the binomial coefficient is given as $\binom{i}{j} = C(i,j) = i!/[j!(i-j)!]$. Inserting the expression of (5) to the second term of (4), and following some algebraic manipulation, we obtain the IF component of the resistive current as

$$i_{r\,\mathrm{if}}(t) \approx \sum_{i=0}^{\infty} (i+1) a_{i+1} \binom{i}{i + \frac{k}{2}} \frac{V_{\mathrm{rf}} V_{lo}^i}{2^i} \times \cos(\omega_{\mathrm{if}} t) + \sum_{i=0}^{\infty} (i+1) a_{i+1} \binom{i}{\frac{i}{2}} \frac{V_{\mathrm{if}} V_{lo}^i}{2^i} \times \cos(\omega_{\mathrm{if}} t + \psi_{\mathrm{if}}). \tag{6}$$

B. Capacitance Mixing

For completeness, the effect of the nonlinear capacitance variations is also considered, although in typical mixer realizations, this is often treated as having a much lower significance and is minimized by using a fully depleted junction or Mott approach (named after N. F. Mott) [1], [4]. Similarly to the nonlinear resistor, the nonlinear capacitance of a pair of Schottky diodes connected antiparallel can be equally generalized into a power series to describe any theoretical or experimentally observed capacitance versus voltage behavior

$$C\Big(V(t)\Big) = \sum_{j=0}^{\infty} C_j V(t)^j \tag{7}$$

where the coefficient of $V(t)^j$, C_j is ideally equal to zero for odd numbers of j's. The unbiased capacitance for the antiparallel Schottky structure is, in essence, contributed by cross-sectional areas of two Schottky devices connected in parallel. In the case of a QBD, however, the capacitance contributed by barriers is, in effect, a series combination of a nonlinear capacitance and a fixed capacitance, which can expressed as

$$C_T\Big(V(t)\Big) = 1 \Bigg/ \left(\frac{1}{C_{do}} + \frac{1}{C_d\Big(V(t)\Big)}\right) \tag{8}$$

where

$$C_{do} = \varepsilon_r \varepsilon_o A / d_o \tag{9}$$

and

$$C_d\Big(V(t)\Big) = \varepsilon_r \varepsilon_o A / d\Big(V(t)\Big). \tag{10}$$

Substituting $V(t) = 0$ to (8) so that $C_d(V(t)) = \infty$, we obtain the unbiased capacitance as $C_T(0) = C_{do}$. Unlike the case of Schottky junctions, where the unbiased capacitance is always determined by two junctions in parallel, the unbiased capacitance of a QBD can be minimized by reducing d_o.

The barrier current can be determined by the time derivative of the instant charge accumulated in the barriers. Since the instant charge $Q(V(t))$ accumulated in the junction is given as

$$Q\Big(V(t)\Big) = C\Big(V(t)\Big) V(t) = \sum_{j=0}^{\infty} C_j V(t)^{j+1} \tag{11}$$

the instant capacitive current as a result of instant change of charge $Q(V(t))$ can be determined simply by

$$i_c(t) = \frac{d\Big(Q\big(V(t)\big)\Big)}{dV(t)} \frac{dV(t)}{dt} = \frac{dV(t)}{dt} \sum_{j=0}^{n} (j+1) C_j V(t)^j. \tag{12}$$

Differentiating (1) with respect to time gives the time derivative of the voltage across the nonlinear capacitance as

$$\frac{dV(t)}{dt} = -\omega_{\rm rf} V_{\rm rf} \sin(\omega_{\rm rf} t) - \omega_{\rm lo} V_{\rm lo} \sin(\omega_{\rm lo} t) + \omega_{\rm if} V_{\rm if} \sin(\omega_{\rm if} t + \psi_{\rm if}). \tag{13}$$

Now, by substituting (13) into (12), and by applying Taylor expansion to the bracketed term of (12) in the similar manner as was done for the nonlinear resistive current, we have

$$\begin{aligned} ic \approx \Big[&-\omega_{\rm rf} V_{\rm rf} \sin(\omega_{\rm rf} t) - \omega_{\rm lo} V_{\rm lo} \sin(\omega_{\rm lo} t) \\ &+ \omega_{\rm if} V_{\rm if} \sin(\omega_{\rm if} t + \psi_{\rm if}) \Big]^* \\ &\times \left[\sum_{i=0}^{\infty} (i+1) C_i V_{\rm LO}(t)^i + \frac{1}{2!} \sum_{i=0}^{\infty} i(i+1) \right. \\ &\left. \times\; C_i V_{\rm LO}(t)^{i-1} \Big(V_{\rm RF}(t) - V_{\rm LO}(t) \Big) \right]. \end{aligned} \tag{14}$$

Now, if we apply (5)–(14) with some algebraic manipulation, the IF mixing product in the capacitive mixing will finally be

$$\begin{aligned} i_{c\,\rm if}(t) = &\;\omega_{\rm if} \sin(\omega_{\rm if} t) \sum_{i=0}^{\infty} i \frac{(i+1) C_i V_{\rm lo}^i V_{\rm if}}{2^i} \binom{i}{i + \frac{k}{2}} \\ &+ \omega_{\rm if} \sin(\omega_{\rm if} t + \psi_{\rm if}) \sum_{i=0}^{\infty} i \frac{(i+1) C_i V_{\rm lo}^i V_{\rm if}}{2^i} \binom{i}{\frac{i}{2}}. \end{aligned} \tag{15}$$

Equation (15) is consistent with (6), except for the fact that the effect of the nonlinear capacitance in (15) is proportionally scaled by the IF frequency.

C. Overall Mixing Equivalent

The total current flowing into the mixing device is the sum of the capacitive current due to the embedding nonlinear capacitance and the resistive current as a result of the embedding nonlinear resistance. That is,

$$\begin{aligned} i_{\rm if}(t) = &\;\omega_{\rm if} \sin(\omega_{\rm if} t) \sum_{i=0}^{\infty} i \frac{(i+1) C_i V_{\rm lo}^i V_{\rm rf}}{2^i} \binom{i}{i + \frac{k}{2}} \\ &+ \omega_{\rm if} \sin(\omega_{\rm if} t + \psi_{\rm if}) \sum_{i=0}^{\infty} i \frac{(i+1) C_i V_{\rm lo}^i V_{\rm if}}{2^i} \binom{i}{\frac{i}{2}} \\ &+ \cos(\omega_{\rm if} t) \sum_{i=0}^{\infty} \frac{(i+1) a_{i+1} V_{\rm rf} V_{\rm lo}^i}{2^i} \binom{i}{i + \frac{k}{2}} \\ &+ \cos(\omega_{\rm if} t + \psi_{\rm if}) \sum_{i=0}^{\infty} \frac{(i+1) a_{i+1} V_{\rm if} V_{\rm lo}^i}{2^i} \binom{i}{\frac{i}{2}}. \end{aligned} \tag{16}$$

Since the load admittance $Y_{\rm if}$ of the IF product harmonic is given as $I_{\rm if} = v_{\rm if} Y_{\rm if}$, with all variables being the phasor quantities, the total current $i_{\rm if}(t)$ can then be expressed as

$$i_{\rm if}(t) = {\rm Re}\{v_{\rm if} Y_{\rm if}\} = {\rm Re}\{v_{\rm if}\} {\rm Re}\{Y_{\rm if}\} - {\rm Im}\{v_{\rm if}\} {\rm Im}\{Y_{\rm if}\}. \tag{17}$$

The phasor $v_{\rm if} = V_{\rm if} \exp(j\psi_{\rm if})$ means that we can express ${\rm Re}\{v_{\rm if}\}$ and ${\rm Im}\{v_{\rm if}\}$, respectively, as ${\rm Re}\{v_{ij}\} = V_{\rm if} \cos(\omega_{\rm if} t + \psi_{\rm if})$ and ${\rm Im}\{v_{\rm if}\} = V_{\rm if} \sin(\omega_{\rm if} t + \psi_{\rm if})$. Thus, (17) becomes

$$i_{\rm if}(t) = V_{\rm if} \cos(\omega_{\rm if} t + \psi_{\rm if}) {\rm Re}\{Y_{\rm if}\} - V_{\rm if} \sin(\omega_{\rm if} t + \psi_{\rm if}) {\rm Im}\{Y_{\rm if}\}. \tag{18}$$

Equating (18) to (16) and with some algebraic rearrangements, we finally obtain the magnitude of the IF voltage, shown in (19), at the bottom of this page, where K_i and K_i' are, respectively, given as $K_i = ((i+1)/2^i)\binom{i}{i+(k/2)}$ and $K_i' = ((i+1)/2^i)\binom{i}{(i/2)}$, and $i + (k/2)$ must be an integer. It follows from (19) that the IF voltage for the second harmonic mixers, i.e., $k = 2$, can be rewritten as (20), shown at the bottom of this page, where $K_i = ((2i+1)/2^{2i})\binom{2i}{i+1}$ and $K_i = ((2i+1)/2^{2i})\binom{2i}{i}$. The embedding impedance of the LO and RF inputs can be evaluated similarly using the above technique of analysis and will be dealt with in a future paper.

D. Implications

In the discussion that follows, the features of the second harmonic mixer using a QBD will be qualitatively derived from (20).

$$V_{\rm if} = V_{\rm rf}^* \sqrt{\frac{\Big(\sum_{i=0}^{\infty} K_i a_{i+1} V_{\rm lo}^i\Big)^2 + w_{\rm if}^2 \Big(\sum_{i=0}^{\infty} K_i C_i V_{\rm lo}^i\Big)^2}{\Big({\rm Re}\{Y_{\rm if}\} + \sum_{i=0}^{\infty} K_i' a_{i+1} V_{\rm lo}^i\Big)^2 + \Big[{\rm Im}\{Y_{\rm if}\} + \omega_{\rm if} \sum_{i=0}^{\infty} K_i' C_i V_{\rm lo}^i\Big]^2}} \tag{19}$$

$$V_{\rm if} = V_{\rm rf}^* \sqrt{\frac{\Big(\sum_{i=0}^{\infty} K_i a_{2i+1} V_{\rm lo}^{2i}\Big)^2 + w_{\rm if}^2 \Big(\sum_{i=0}^{\infty} K_i C_{2i} V_{\rm lo}^{2i}\Big)^2}{\Big({\rm Re}\{Y_{\rm if}\} + a_1 + \sum_{i=1}^{\infty} K_i' a_{2i+1} V_{\rm lo}^{2i}\Big)^2 + \Big[{\rm Im}\{Y_{\rm if}\} + \omega_{\rm if} \Big(C_0 + \sum_{i=1}^{\infty} K_i' C_i V_{\rm lo}^{2i}\Big)\Big]^2}} \tag{20}$$

1) Voltage-Independent Admittance: The denominator of (20) contains two voltage-independent terms related to the nonlinearities intrinsic to the device, i.e., a_1 and $\omega_{\text{if}}C_0$. Like the parasitic burden to a network, the effect of a_1 and C_0 is to reduce the IF voltage, thereby degrading the Q factor of the device. a_1 and C_0 represent, respectively, the linear conductance and unbiased capacitance of the device. Mathematically speaking, a polynomial $P(z) = p_0 + p_1 z + p_2 z^2 + \cdots + p_n z^n$ will behave like $p_0 + p_1 z$ or $p_0 + p_m z^m$, with $m \geq 1$, for a very small value of $|z|$. Accordingly, when a second subharmonic mixer is pumped at a very low LO voltage, it is expected that (20) will behave like (21), shown at the bottom of this page, which means the effect of the linear conductance and unbiased capacitance is particularly dominant at a very low LO pump.

Now, if the capacitance effect is suppressed, either by applying the correct IF admittance or by using a relatively low IF frequency, (21) can be simplified as

$$V_{\text{if}} = V_{\text{rf}} \frac{K_1}{\dfrac{\text{Re}\{Y_{\text{if}}\} + a_1}{a_3 V_{\text{lo}}^2} + K_1'}. \tag{22}$$

By direct inspection of (22), while the presence of voltage-independent conductance in the device is to reduce the IF voltage at low LO application, the role of a_3 is to scale up the effect of the LO power, which monotonically increases the IF power until it reaches the NDR region. The behavior of (22) is best illustrated by Fig. 2, which shows a graph of IF power versus LO power at different LO frequencies.

2) First Minimum Conversion Loss: If the LO power is further increased beyond the negative differential resistance (NDR) regions of the *I–V* characteristic, the approximation of (21) and (22) will no longer be valid. However, for the sake of prediction of the mixing behavior at low LO application, we can still apply the appropriate approximation to describe the behavior to the first order, without over sacrificing accuracy. We can approximate (22), say, by incorporating the next higher order effect into the equation, as

$$V_{\text{if}} \approx V_{\text{rf}} \frac{\dfrac{3}{4} a_3 V_{\text{lo}}^2 + \dfrac{5}{4} a_5 V_{\text{lo}}^4}{\Big(\text{Re}\{Y_{\text{if}}\} + a_1\Big) + \dfrac{3}{2} a_3 V_{\text{lo}}^2 + \dfrac{15}{8} a_5 V_{\text{lo}}^4}. \tag{23}$$

Equating $dV_{\text{if}}/V_{\text{lo}}$ to zero, from which we obtain the LO voltage leads to the first minimum IF voltage shown in (24), at the bottom of the following page. If a_5 is negative so that it accounts for the existence of the NDR regions in the *I–V* characteristic, it can be seen by direct inspection of (24) that a greater magnitude of a_5 will result in lower LO voltage required to attain the first minimum in the IF voltage. Mathematically speaking, the greater the magnitude of any negative coefficient of the lowest order, such as a_5 in this instance, implies that the NDR regions will be closer to the origin of the *I–V* characteristic. It follows that lower LO power will be required to reach the first minimum in conversion loss if the NDR regions are drawn closer to the y-axis of the *I–V* characteristic.

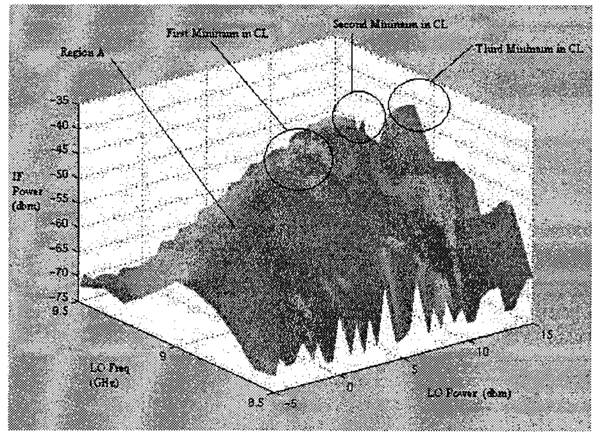

(a)

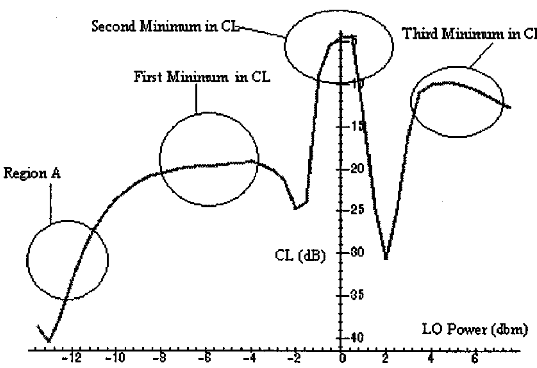

(b)

Fig. 2 (a) Measured IF power versus LO power characteristic. (b) Simulated conversion loss versus LO power (CL = conversion loss).

3) Implications of Multiple Minima in Conversion Loss: Another interesting point is the multiple minima in conversion loss, as seen both analytically and experimentally. Assuming that the nonlinear capacitance effect is properly suppressed, we can approximate (25) by taking off the capacitance associated terms in the following manner:

$$V_{\text{if}} = V_{\text{rf}}^* \sqrt{\frac{\left(\sum_{i=0}^{\infty} K_i a_{i+1} V_{\text{lo}}^i\right)^2}{\left(\text{Re}\{Y_{\text{if}}\} + a_1 + \sum_{i=1}^{\infty} K_i' a_{i+1} V_{\text{if}}^i\right)^2}}. \tag{25}$$

$$V_{\text{if}} \cong V_{\text{rf}} \sqrt{\frac{\Big[K_1 a_3 V_{\text{lo}}^2\Big]^2 + \Big[\omega_{\text{if}} K_1 b_2 V_{\text{lo}}^2\Big]^2}{\Big[\text{Re}\{Y_{\text{if}}\} + a_1 + K_1' a_3 V_{\text{lo}}^2\Big]^2 + \Big[\text{Im}\{Y_{\text{if}}\} + \omega_{\text{if}}\Big(b_0 + K_1' b_2 V_{\text{lo}}^2\Big)\Big]^2}} \tag{21}$$

The maximum or the minimum IF voltage can be determined by differentiating (25) with respect to LO voltage V_{lo}, which gives (26), shown at the bottom of this page. It can be proven algebraically by expansion of (26) that the bracketed expression $(rK_sK_r' - sK_s'K_r)$ of the right-hand side is always positive in value. It follows that, if the value of $dV_{\mathrm{if}}/dV_{\mathrm{lo}}$ is to be zero, there will be no positive real root for V_{lo} unless the sign of a_j happens to be negative for some j's. In the case of a QBD, the sign of a_j in the power series given in (2) can be negative for some j's, which result from the negative dynamic conductance's in the VI characteristic. It suffices to prove the existence of multiple minima in conversion loss in the case of the QBD. For Schottky junctions, however, the sign of the coefficients a_j of their power series representations (as are rigidly determined by the exponential relationship) are positive for all j's. This means that, for a two-tone excitation, the IF voltage in the Schottky junction can only increase monotonically with the increase in the LO voltage. Thus, the multiple–minimum conversion-loss characteristic is one of the unique features of the QBD that is not found in an ideal Schottky junction.

The feature of multiple minima in conversion loss can be graphically illustrated in Fig. 2(a) and (b). It can be observed that after the first minimum in conversion loss, there exist a second and third minimum. The conversion losses of the second and third minimum are much lower than that of the first minimum. The NDR region, coupled with the higher order nonlinearities, generates subharmonic components, which effectively image enhances the IF power, thereby minimizing the conversion loss.

III. Measurements

This section presents measurements with regard to the mixing performance of a range of QBD's with different device characteristics taken from molecular-beam-epitaxial layer alternatives.

The test fixture employed for this investigation was a subharmonically pumped down-converter [9], which is shown in Fig. 3. This mixer was designed to down-convert an RF signal at 18–19 GHz to an IF of around 900 MHz, with the LO input being subharmonically driven at around 8.5–9.5 GHz. This is a frequency-scaled analog for a future realization at a frequency of ten times higher.

Case 1: Device of 10 μm in Diameter Calculated Voltage-Independent Conductance $=$ 0.0016 mho. Fig.4(a) shows the measured *I–V* characteristic of the QBD of 10 μm in diameter based on a device featuring two 4.3-nm $Al_{0.4}Ga_{0.6}As$ barriers separated by a 5.1-nm GaAs well. By calculation, the voltage-independent conductance was found to be 0.0016 mho. The best conversion loss was around 5 dB, when the LO power was at around 0.8 dBm. When the LO power is reduced to around -2 dBm, the conversion loss is still less than 10 dB, which is equivalent to the first minimum that we discussed previously. The measured IF power versus IF frequency for LO Power $=$ 0 dBm, RF Power $= -20$ dBm, shown in Fig.4(b).

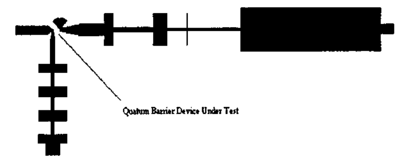

Fig. 3 Layout of the 18–1-GHz subharmonic mixer (not to scale).

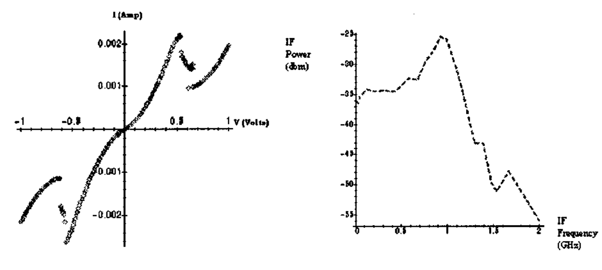

(a) (b)

Fig. 4 (a) Measured *I–V* characteristic of QBD of 10 μm in diameter (voltage-independent conductance $= 0.0016$). (b) Measured IF power against LO frequency for LO power $=$ 0 dBm, RF frequency $=$ 18 GHz, RF power $= -20$ dBm.

Case 2: Device of 10 μm in Diameter Calculated Voltage-Independent Conductance $= 0.024$ mho. Fig. 5(a) shows the measured *I–V* characteristic of the device featuring two 1.7-nm AlAs barriers separated by a 4.3-nm GaAs well. The device diameter is the same as that in case 1, but the current densities are different. The *I–V* characteristic of this device differs from the one in case 1 in that the NDR region of this case is much further away from the origin. The measured IF power versus LO frequency is shown in Fig. 5(b) for different LO powers. As can be observed from Fig. 5(b), the device seems to be operating below the NDR regions, where the conversion loss decreases with the

$$V_{\mathrm{lo}}^2 = \frac{-80\left(a_1 + \mathrm{Re}\{Y_{\mathrm{if}}\}\right) + \sqrt{400\left(a_1 + \mathrm{Re}\{Y_{\mathrm{if}}\}\right)^2 - 90a_3^2\left(a_1 + \mathrm{Re}\{Y_{\mathrm{if}}\}\right)^{\frac{90a_3^2\left(a_1 + \mathrm{Re}\{Y_{\mathrm{if}}\}\right)}{a_5}}}}{30a_3} \tag{24}$$

$$\frac{dV_{\mathrm{if}}}{dV_{\mathrm{lo}}} \approx V_{\mathrm{rf}} \frac{\sum_{i=1}^{\infty} 2iK_i a_{2i+1} V_{\mathrm{lo}}^{2i-1}\left[a_1 + \mathrm{Re}\{Y_{\mathrm{if}}\}\right]}{\left(\mathrm{Re}\{Y_{\mathrm{if}}\} + a_1 + \sum_{i=0}^{\infty} K_i' a_{2i+1} V_{\mathrm{lo}}^{i}\right)^2} + V_{\mathrm{rf}} \frac{\left\{\sum_{r=1}^{\infty}\sum_{s=1}^{\infty} 2\left(rK_sK_r' - sK_s'K_r\right) a_{2r+1} a_{2s+1} V_{\mathrm{lo}}^{2r+2s-1}\right\}}{\left(\mathrm{Re}\{Y_{\mathrm{if}}\} + a_i + \sum_{i=0}^{\infty} K_i' a_{2i+1} V_{\mathrm{lo}}^{2i}\right)^2} \tag{26}$$

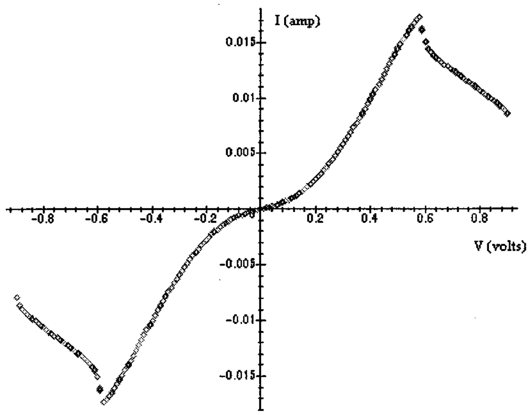

(a)

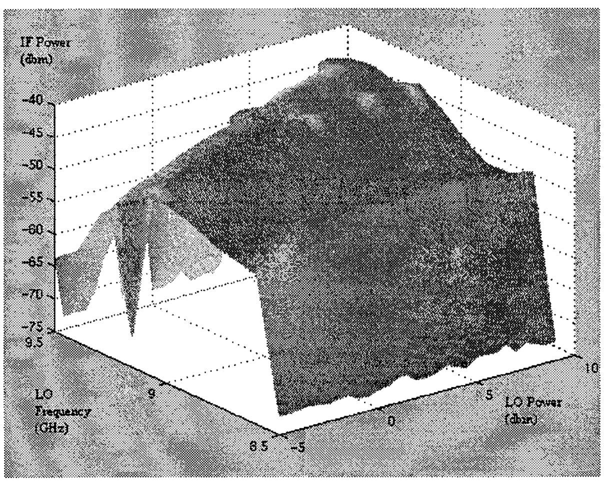

(b)

Fig. 5 (a) Measured *I–V* characteristic of QBD of 10 μm in diameter (voltage-independent conductance $= 0.024$). (b) Measured IF power against LO frequency for different LO power, RF frequency $= 18$ GHz, RF power $= -23$ dBm.

rise in the LO power. The conversion efficiency is inferior to that in case 1 due to higher degree of voltage independence.

The previous analysis, coupled with the actual measurements, generates a number of hints leading to the improvement of the intrinsic conversion efficiency or lower LO requirement. To maintain a reasonable LO efficiency for low LO operation, the voltage-independent conductance and unbiased capacitance should be minimized. On the other hand, the NDR region should be drawn as close to the y-axis as possible so that less LO power is required to reach, or go beyond, the first minimum in conversion loss. There is no question that the unbiased capacitance can be reduced simply by selection of a device of smaller diameter. However, the lower the voltage-independent conductance as well as the closer the NDR regions to the y-axis will need to be achieved by selection of suitable layer structures during fabrication. This can and has been achieved by structures with increased well widths and with coupled quantum wells that have already been grown and await evaluation in similar mixers.

IV. Conclusion

In this paper, a qualitative treatment has been given to identify the significant effect of the location of the negative dynamic resistance regions: the voltage-independent conductance and capacitance intrinsic to a QBD on second harmonic mixing. Measurements of the mixing performance based on two devices of different current densities and layer structures have been made to validate some of our initial observations from this study. Research is in progress to perform further measurements to identify the effect of the device level nonlinearities, which are required for subharmonic mixing with an optimal conversion efficiency and to understanding the layer structure factors that alter the carrier supply function. These factors, in turn, greatly affect the nonlinear behavior of the current versus voltage characteristic, and can be used to achieve low conversion loss with very low levels of LO signal. This is especially appealing at submillimeter-wave frequencies and beyond.

Acknowledgment

The authors wish to thank Dr. M. Henini, Department of Physics, University of Nottingham, Nottingham, U.K., for the growth of the molecular beam epitaxy (MBE) material.

References

[1] N. F. Mott, “Note on the contact between a metal and an insulator or semiconductor,” in *Proc. Cambridge Philosophical Soc.*, 1938, p. 568.
[2] J.-D. Buchs and G. Begemann, “Frequency conversion using harmonic mixers with resistive diodes,” *IEEE J. Microwave Opt. Acoust.*, vol. MOA-2, pp. 71–76, May 1978.
[3] M. Cohn, J. E. Degenford, and B. A. Newman, “Harmonic mixing with an antiparallel diode pair,” *IEEE Trans. Microwave Theory Tech.*, vol. MTT-23, pp. 667–673, Aug. 1975.
[4] S. A. Maas, *Microwave Mixers*, 2nd ed. Norwood, MA: Artech House, 1993.
[5] R. J. Malik and S. Dixon, “A subharmonic mixer using a planar doped barrier diode with symmetric conductance,” *IEEE Electron Device Lett.*, vol. EDL-3, pp. 205–207, July 1982.
[6] G. Millington, R. E. Miles, R. D. Pollard, D. P. Steenson, and J. M. Chamberlian, “A resonant tunneling diode self-oscillating mixer with conversion gain,” *IEEE Microwave Guided Wave Lett.*, vol. 1, pp. 320–321, Nov. 1991.
[7] S. A. Mass, *Microwave Mixers*. Norwood, MA: Artech House, 1993, pp. 226–227.
[8] G. B. Tait, “Microwave mixers employing multiple-barrier semiconductor heterostructure devices,” *IEEE Trans. Microwave Theory Tech.*, vol. 42, pp. 1596–1601, Sept. 1994.
[9] W. Y. Liu and D. P. Steenson, “18-to-1 GHz subharmonically pump downconverter using a quantum barrier device with symmetric conductance,” Inst. Elect. Eng., U.K., Jan. 1999.
[10] R. A. Kiehl, T. C. L. G. Sollner, and H. C. Liu, “High-frequency resonant-tunneling devices in high-speed heterostructure devices,” in *Semiconductors & Semimetals*, R. K. Willardson, A. C. Beer, and E. R. Weber, Eds. New York: Academic, 1994.

W. Y. Liu (M’98) received the B.Sc. degree in electrical engineering from The University of Sunderland, Sunderland, U.K., in 1989, and is currently working toward the Ph.D. degree at The University of Leeds. Leeds, U.K.

He is a consultant on Cadence to Micro Logic Design Inc., San Jose, CA.

David Paul Steenson (M'96) received the B.Sc. degree in electronics and electrical engineering from the University of Manchester Institute of Science and Technology (UMIST), Manchester, U.K., in 1984, and the Ph.D. degree from the University of Nottingham, Nottingham, U.K., in 1993.

In 1984, he joined Philips Components, Stockport, Cheshire, U.K., as a Microwave Device Development Engineer. He later joined the Philips Research Laboratories, Surrey, U.K., to work on the development of monolithic microwave integrated circuits. In 1989, he joined the Department of Physics, University of Nottingham, to conduct research into the high-frequency applications of double-barrier resonant tunneling devices (DBRTD's). In 1993, he joined the Department of Electronic and Electrical Engineering, The University of Leeds, where he continued to investigate the high-frequency applications of DBRTD's. In 1994, he became a permanent faculty member, working at the Institute of Microwaves and Photonics, School of Electronic and Electrical Engineering, The University of Leeds. His research interests are in the exploitation of novel electronic devices and principles for millimeter- and submillimeter-wave subsystems.